Cu−Dinitrosyl Species in Zeolites: A Density Functional Molecular Cluster Study

R. Ramprasad,[†] K. C. Hass,[‡] W. F. Schneider,*[,‡] and J. B. Adams[§]

Department of Materials Science and Engineering, University of Illinois, Urbana, Illinois 61801, Ford Research Laboratory, MD 3083/SRL, Dearborn, Michigan 48121-2053, and Department of Chemical, Biological and Materials Engineering, Arizona State University, Tempe, Arizona 85287

Received: August 30, 1996; In Final Form: March 31, 1997[⊗]

A small cluster model proposed earlier to examine bound Cu ions and their interaction with CO and NO in zeolites [Schneider, W. F.; Hass, K. C.; Ramprasad, R.; Adams, J. B. *J. Phys. Chem.* **1996**, *100*, 6032] is used to study Cu-bound dinitrosyl complexes. The possibility of a single-step, symmetric, concerted reaction occurring between the two nitrosyl ligands to form either a N−N bond or free N_2 and O_2 is addressed. Density functional theory is used to predict molecular and electronic structures and binding energies. N-down dinitrosyl binding to Cu^0, Cu^+, and Cu^{2+} can be represented as $[Cu(I)-(NO)_2^-]$, $[Cu(I)-(NO)_2]$, and $[Cu(I)-(NO)_2^+]$, respectively, with the dinitrosyl moiety closely resembling the free NO dimer, and having a long N−N bond (≈2.8 Å). Dinitrosyl species bound to Cu through the O display two distinct binding modes, one resembling the N-down dinitrosyl binding, again with a long N−N bond (≈2.0 Å), and the other similar to hyponitrite binding to a metal atom, displaying a short N−N bond (≈1.2 Å). The single-step, symmetric, concerted decomposition reaction of NO in the vicinity of Cu ion sites in zeolites is forbidden by orbital symmetry and is anticipated to have a comparable or higher activation barrier than the same reaction in the gas phase. Metastable hyponitrite complexes, on the other hand, display N−N coupling and may be precursors for a multistep decomposition of NO in the presence of Cu-exchanged zeolites.

I. Introduction

Although thermodynamically unstable to decomposition to N_2 and O_2 (reaction 1), free NO is unusually kinetically stable.[1,2]

$$2NO \rightarrow N_2 + O_2 \qquad (1)$$

The concerted decomposition reaction, passing through a cyclic transition state, is symmetry forbidden,[2,3] and under extreme conditions, reaction 1 instead occurs via a sequence of high-energy atom exchange reactions.[4]

Cu-exchanged zeolites, in particular Cu-ZSM-5, have the highest known activities for catalyzing reaction 1,[5,6] as well as for the closely related selective catalytic reduction (SCR) of NO in net oxidizing gas streams.[5−7] Despite considerable experimental effort aimed at understanding this catalytic activity,[8−31] many questions remain regarding both the NO decomposition and SCR mechanisms. Speculations on these mechanisms are based primarily on experimentally identifiable $Cu-N_xO_y$ complexes. In particular, Cu−*gem*-dinitrosyl species have been suggested to play a direct role in N−N bond formation,[5,10,13,16] possibly by promoting the concerted, direct decomposition to N_2 and O_2. In this work, we use density functional theory to identify and characterize the stable and meta-stable Cu−dinitrosyl species possible in Cu-exchanged zeolites and assess the likelihood of their involvement in this direct decomposition reaction.

Cu-exchanged zeolites can contain a mixture of Cu^+ and Cu^{2+} ions, coordinated to the zeolite lattice and charge compensated by anionic Al T-sites and possibly, in the case of Cu^{2+}, by extralattice ions, such as O^- and OH^-.[5,21] The zeolite lattice relaxes locally to accommodate the bare or ligated Cu ion, but the lattice structure itself remains essentially unaltered.[32] Both Cu^+ and Cu^{2+} sites are observed to adsorb single NO molecules, while only Cu^+ appears to support the formation of *gem*-dinitrosyl species.[9−11,13−17] The tendency of NO to adsorb in pairs has been observed on many transition metal oxide surfaces and transition metal ion exchanged zeolites,[33,34] and has been ascribed to enhanced stability gained by the interaction of the unpaired electron on each of the NO ligands.[35]

Because of the absence of detailed information as to the location of exchanged Cu ions, and the probable absence of unique Cu sites, we have chosen in this and previous studies[36−38] to consider very simple models of Cu ions exchanged in zeolites that focus primarily on the oxidation state and the immediate coordination environment of the Cu ion. Thus, the coordination of Cu to its nearest neighbor framework oxygen atoms (modeled using water ligands) and adsorbed gas molecules (*viz.*, NO) are treated explicitly. Symmetry constraints are imposed to maintain "zeolite-like" coordination, and geometry optimizations within these constraints are performed to simulate the relaxation of the zeolite lattice and adsorbates. Clearly, these simple models neglect some important details of the zeolite environment, but these simplifications allow a focus on the qualitative characteristics of the Cu−NO interactions. In fact, previous studies of adsorbates on zeolite-bound Cu indicate that the use of more sophisticated zeolite models produces only minor perturbations on the *dominant* effects modeled here.[36−41] Recently, a number of larger cluster—albeit less comprehensive—calculations for Cu−dinitrosyl species have been reported.[42,43]

This paper is organized as follows. Section II outlines the computational approach. Section III presents results for neutral and anionic free NO dimers. In section IV, the geometric and electronic structures and binding energies of the Cu−dinitrosyl complexes are explored. A surprising richness of dinitrosyl binding modes is found, including both N-down and O-down *gem*-dinitrosyl and hyponitrite species. While the N−N separa-

* Author to whom correspondence should be addressed.
[†] University of Illinois.
[‡] Ford Research Laboratory.
[§] Arizona State University.
[⊗] Abstract published in *Advance ACS Abstracts,* August 1, 1997.

S1089-5647(96)02706-X CCC: $14.00

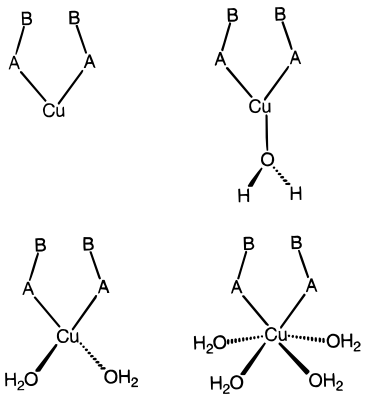

Figure 1. Schematic structures of Cu-bound dinitrosyl $[Cu(H_2O)_x(NO)_2]^{n+}$ (A = N, B = O) and $[Cu(H_2O)_x(ON)_2]^{n+}$ (A = O, B = N) complexes for $x = 0$, 1, 2, or 4.

tion in the dinitrosyl complexes is always >2 Å, it is only 1.2−1.3 Å in the hyponitrite-like complexes. In section V, the basic features of the Cu−dinitrosyl equilibrium geometries are explained. Finally, in section VI, we review the symmetry-forbidden nature of the concerted decomposition of free NO to N_2 and O_2 and consider whether the N-down or O-down binding of the NO to a zeolite-bound Cu ion can catalyze this reaction or otherwise promote the formation of an N−N bond.

II. Computational Details

Calculations were performed using the Amsterdam Density Functional (ADF)[44] code with all options as chosen in ref 38. A split-valence plus polarization Slater orbital basis set was used for all main group elements, and a double-zeta s and p and triple-zeta d Slater orbital basis was used for Cu. Unless otherwise stated, equilibrium geometries were obtained within the local spin density approximation (LSDA)[45] by gradient optimizations. Geometries were considered converged when the maximum and the rms forces were less than 0.001 hartrees/bohr. Improved binding and orbital energies were obtained in all cases by the inclusion of Becke exchange[46] and Perdew correlation[47] gradient corrections (BP86), usually in single-point calculations at the LSDA geometries. A reasonably conservative integration mesh parameter (which controls the accuracy of the Hamiltonian matrix elements) of 4.5 was used throughout.[48]

The model Cu−dinitrosyl complexes considered here are sketched in Figure 1. They are of the general form $[Cu(H_2O)_x(NO)_2]^{n+}$, $x = 0$, 1, 2, 4, $n = 0-2$, for N-down binding of the two nitrosyl ligands to Cu, and $[Cu(H_2O)_x(ON)_2]^{n+}$ for O-down binding. All complexes were constrained to C_{2v} symmetry (except $[Cu(NO)_2]^{n+}$, $n = 0-2$, for which the possible $D_{\infty h}$ linear geometry, not shown in Figure 1, was also examined) and were assigned a 0, 1+, or 2+ charge. The actual coordination of Cu ions to framework oxygen atoms in high-silica zeolites like Cu-ZSM-5 is not firmly established. Available theoretical[36,37,39] and experimental[28−31] evidence suggests that Cu^+ prefers to be coordinated to about two framework oxygen atoms and Cu^{2+} prefers a somewhat higher coordination. In the present study, we consider a range of possible coordination of Cu to framework oxygen, both to examine trends that accompany increasing Cu coordination and because of the uncertainties in the Cu environment in zeolites. Cu was coordinated to 0, 1, 2, or 4 water ligands, with the plane of the dinitrosyl species between adjacent water ligands ($x > 1$) or between O−H vectors ($x = 1$).[49] For several selected cases, the C_{2v} symmetry constraint was relaxed so that the two nitrosyl ligands become symmetry inequivalent. In such cases, the complexes reverted back to the C_{2v} structures, indicating a preference for this symmetry.

III. Neutral and Anionic NO Dimers

The spontaneous dimerization of NO has been observed in both condensed and gas phases;[50−52] experimental estimates for the dissociation energy of free $(NO)_2$ (to two NO molecules) range between 1.5 and 3.7 kcal mol^{-1}.[51,53,54] This very weak interaction is difficult to describe theoretically, with results varying significantly with the type of electron correlation treatment.[55−58] Experimental estimates of the geometry vary significantly with the type of experiment,[51,52] and some uncertainty even exists as to whether the ground state of the dimer is a singlet or triplet.[55] In Table 1, we list the BP86 geometries and dissociation energies (with respect to the NO ($^2\Pi$) + NO ($^2\Pi$) asymptote) for the singlet ($^1A_1$) and the triplet ($^3B_1$) states of the *cis* and *trans* forms of $(NO)_2$. The *cis*-triplet state is found to be the most stable, with the *cis*-singlet about 5 kcal mol^{-1} higher in energy. As shown on the left side of Figure 2 for the *cis*-triplet, the NO dimer electronic structure derives primarily from symmetric and antisymmetric combinations of individual NO levels, with some mixing between 5σ and in-plane 1π levels. For instance, the π_1 and π_4 levels are the symmetric and antisymmetric combinations of the in-plane NO 2π levels, respectively, and the π_2 and π_3 levels are those of the out-of-plane NO 2π levels. Most of the structures exhibit long N−N separations (≈2 Å), reflecting the net weak bonding mediated by the NO 2π combinations. For comparison, typical N−N single, double and triple bond separations are 1.45 Å (in N_2H_4), 1.21 Å (in N_2F_2), and 1.09 Å (in N_2), respectively.[61] The one exception to the long N−N separation is the ^1A_g *trans* structure, whose electronic structure derives from double occupation of one of the out-of-plane NO 2π combinations. The geometric parameters and the relative ordering and magnitude of energies for the different structures are in good agreement with earlier density functional studies.[55,59]

Reduction of $(NO)_2$ by one or two electrons considerably alters both its electronic and geometric structures. The BP86 optimized geometries and relative energies for the *cis* and *trans* forms of $N_2O_2^-$ and $N_2O_2^{2-}$ are listed in Table 1. To our knowledge, the only previously reported study of these anions is for the higher energy NNO_2^- geometric isomer.[60] *Trans*-$N_2O_2^-$ is more stable than the *cis* conformer, while the opposite is true for $N_2O_2^{2-}$. The N−N bond lengths of $N_2O_2^-$ and $N_2O_2^{2-}$ are typical of metal hyponitrites (1.2−1.3 Å),[50,62] and are considerably shorter than that in the neutral dimer. We focus here on the *cis* forms relevant to the Cu systems discussed below.

The electronic structure of *cis*-$^3B_1$ $N_2O_2^-$, shown schematically in the center of Figure 2, is obtained by adding a second electron to the π_1 orbital of $(NO)_2$; this reduction drives a decrease in N−N separation (to 1.48 Å) and increase in N−O separations consistent with the character of the π_1 level. The largely N−N antibonding $2b_2$ level is driven up in energy by the decrease in N−N separation, and transfer of an electron from this to the $2b_1$ orbital generates the $^2B_2$ state, which has an even shorter optimal N−N separation (1.23 Å) and longer N−O separations. Reduction by a second electron produces the closed-shell *cis*-$N_2O_2^{2-}$ (hyponitrite) anion, shown on the right of Figure 2. In all these anions, electron density accumulates on the O centers, in particular in the $2b_2$ level, which rehybridizes in such a fashion to make it ideally suited to interact with the d orbitals of a chelated metal atom. In fact, as we will see in subsequent sections, an electron-rich metal center can drive the reduction of two O-down NO ligands and the formation of a short N−N bond. The charge accumulation at the O centers, and accompanying decrease in N−N separation,

TABLE 1: Calculated Properties (BP86) for the *cis* and *trans* Forms of Free $(NO)_2$, $N_2O_2^-$, and $N_2O_2^{2-}$: Bond Lengths in Angstroms, Bond Angles in Degrees, and Energies in kcal mol^{-1}

	cis-$(NO)_2$		*trans*-$(NO)_2$			*cis*-$N_2O_2^-$		*trans*-$N_2O_2^-$	*cis*-$N_2O_2^{2-}$	*trans*-$N_2O_2^{2-}$
	$^1A_1$	$^3B_1$	^1A_g	^3A_u	^1A_g	$^2B_2$	$^2B_1$	^2A_g	$^1A_1$	^1A_g
N−N	2.080	2.049	1.986	1.979	1.196	1.228	1.481	1.316	1.310	1.311
N−O	1.165	1.167	1.170	1.167	1.225	1.348	1.271	1.295	1.398	1.414
N−N−O	97.1	108.1	107.5	112.1	146.8	117.3	114.4	121.7	121.7	112.1
E	−14[a]	−19[a]	−8[a]	−18[a]	−11[a]	+9[b]	+2[b]			+2[c]

[a] Energy of reaction $2NO \rightarrow (NO)_2$. [b] Energy relative to ^2A_g *trans*-$N_2O_2^-$. [c] Energy relative to $^1A_1$ *cis*-$N_2O_2^{2-}$.

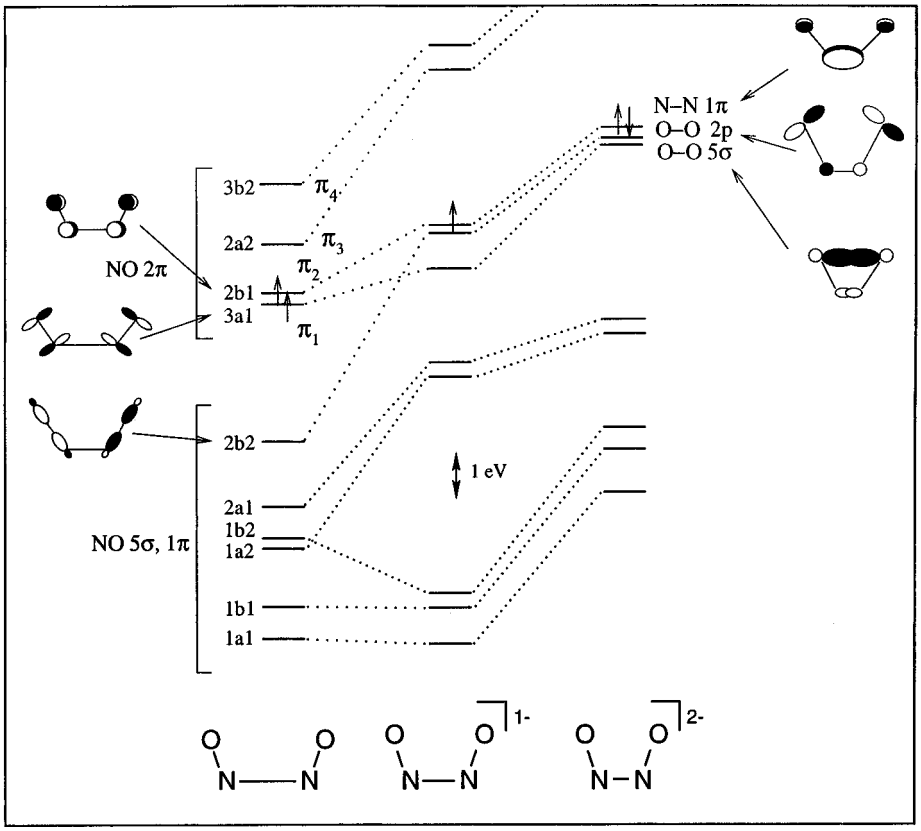

Figure 2. Schematic molecular orbital diagrams for $^3B_1$ *cis*-$(NO)_2$ (left), $^3B_1$ *cis*-$N_2O_2^-$ (center), and $^1A_1$ *cis*-$N_2O_2^{2-}$ (right). Levels below those indicated by arrows are all doubly occupied, and those above are empty.

is perhaps best illustrated by the Lewis diagrams for the neutral dimer and hyponitrite anion:

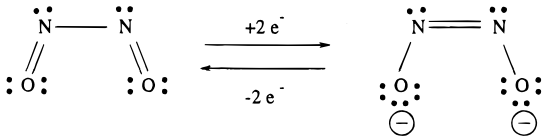

IV. Minimum Energy Structures for Cu−Dinitrosyl Complexes

A. N-Down Structures. We now examine the equilibrium geometries, electronic structure, and binding energies of N-down Cu−dinitrosyl complexes ($[Cu(H_2O)_x(NO)_2]^{n+}$, $n = 0, 1, 2$). The high degree of covalency in the Cu−$(NO)_2$ interaction makes assignment of the Cu oxidation state in these complexes somewhat ambiguous. Using the notation of Enemark and Feltham,[36,64] the dinitrosyl systems with overall charges of 0, 1+, and 2+ can be described as $\{Cu(NO)_2\}^{13}$, $\{Cu(NO)_2\}^{12}$, and $\{Cu(NO)_2\}^{11}$, respectively, where the superscript indicates the total number of electrons in the Cu d and NO 2π levels. For each electron count we consider first the bare $[Cu(NO)_2]^{n+}$ complexes, which illustrate the essential features of the Cu−$(NO)_2$ interactions, and then consider the peturbations introduced by including water ligands. The important structural parameters for these complexes are summarized in Table 2. In all cases examined here, the two NO ligands adopt equivalent conformations; that is, we find no tendency for formation of a mixed linear−bent dinitrosyl complexes such as those found for early transition metal dinitrosyl species.[65−68]

$[Cu(H_2O)_x(NO)_2]^{2+}$. Both linear ($D_{\infty h}$) and bent (C_{2v}) $[Cu(NO)_2]^{2+}$ minima exist, with the latter more stable by 5.0 kcal mol^{-1}. A curious feature of the bent structure is a leaning inward of the two NO ligands toward each other, so that the O−O separation is less than the N−N separation; the latter separation is even longer than in free $(NO)_2$. This bonding motif persists in all the N-down dinitrosyl species considered here, and we will consider its origin in section V. Only the bent structure persists when additional ligands are added to Cu, and we focus on this conformation. The electronic structure of $^2A_1$ $[Cu(NO)_2]^{2+}$ (Figure 3a) is strikingly similar to that of the free NO dimer, with the Cu d levels inserted between orbitals of NO $5\sigma/1\pi$ and of NO 2π origin. A single electron is transfered to the Cu d from the NO 2π manifold, reflecting a partial reduction of Cu and oxidation of the NO ligands, accompanied by a shortening of the N−O bond. The electronic structure can thus be represented as $[Cu(I)-(NO)_2^+]$. A similar reduction of Cu^{2+} by a single NO ligand has been noted previously.[36]

TABLE 2: Selected LSDA Geometric Parameters, Cu d Population and BP86 Fragmentation Energies for $[Cu(H_2O)_x(NO)_2]^{n+}$ Complexes: Bond Lengths in Angstroms, Bond Angles in Degrees, and Energies in kcal mol^{-1}

	state	Cu−N	N−N	N−O	O−O	Cu−O_H	N−Cu−N	Cu−N−O	Cu d pop.	E^a
					Cu^{2+} Systems ($n = 2$)[b]					
$x = 0$	$^2\Pi_g$	1.855	3.710	1.102	5.914		180.0	180.0	9.65	−216.4
$x = 0$	$^2A_1$	1.959	3.688	1.103	2.866		140.6	142.0	9.68	−221.4
$x = 1$	$^2A_1$	1.968	2.778	1.111	2.698	1.896	89.8	133.0	9.59	−271.7
$x = 2$	$^2A_1$	1.987	2.713	1.116	2.499	1.954	86.1	131.5	9.55	−311.8
$x = 4$	$^2A_1$	2.028	2.735	1.121	2.470	2.163	84.8	130.8	9.65	−350.7
					Cu^{+} Systems ($n = 1$)					
$x = 0$	$^1A_1$	1.947	2.865	1.141	2.274		94.8	117.6	9.67	−68.2
$x = 1$	$^1A_1$	1.926	2.713	1.147	2.223	1.935	89.6	122.9	9.63	−99.6
$x = 2$	$^1A_1$	1.899	2.642	1.153	2.216	2.032	88.2	125.3	9.58	−118.5
$x = 4$	$^1A_1$	1.903	2.656	1.158	2.231	2.218	88.5	125.2	9.62	−129.9
$x = 0$	$^3\Sigma_g^-$	1.732	3.464	1.138	5.740		180.0	180.0	9.53	−68.4
$x = 0$	$^3B_1$	1.871	2.816	1.146	2.626		98.5	126.0	9.65	−59.6
$x = 1$	$^3B_1$	1.861	2.618	1.149	2.492	1.933	89.4	132.2	9.62	−94.7
$x = 2$	$^3B_1$	1.870	2.619	1.154	2.455	2.046	88.8	131.5	9.60	−113.3
$x = 4$	$^3B_1$	1.921	2.613	1.159	2.356	2.237	85.7	130.8	9.66	−123.0
					Cu^{0} Systems ($n = 0$)					
$x = 0$	$^2\Pi_u$	1.679	3.358	1.176	5.710		180.0	180.0	9.45	−58.9
$x = 0$	$^2B_1$	1.874	2.904	1.184	2.244		101.6	113.0	9.65	−59.3
$x = 1$	$^2B_1$	1.869	2.730	1.189	2.182	2.011	93.8	119.8	9.65	−70.3
$x = 2$	$^2B_1$	1.860	2.704	1.194	2.192	2.171	93.3	121.0	9.64	−75.9
$x = 4$	$^2B_1$	1.887	2.689	1.196	2.237	2.312	90.9	123.7	9.64	−76.7

[a] Energy of reaction $Cu^{n+} + xH_2O + 2NO \rightarrow [Cu(H_2O)_x(NO)_2]^{n+}$. [b] Energy referenced to spherically averaged Cu^{2+} ion.

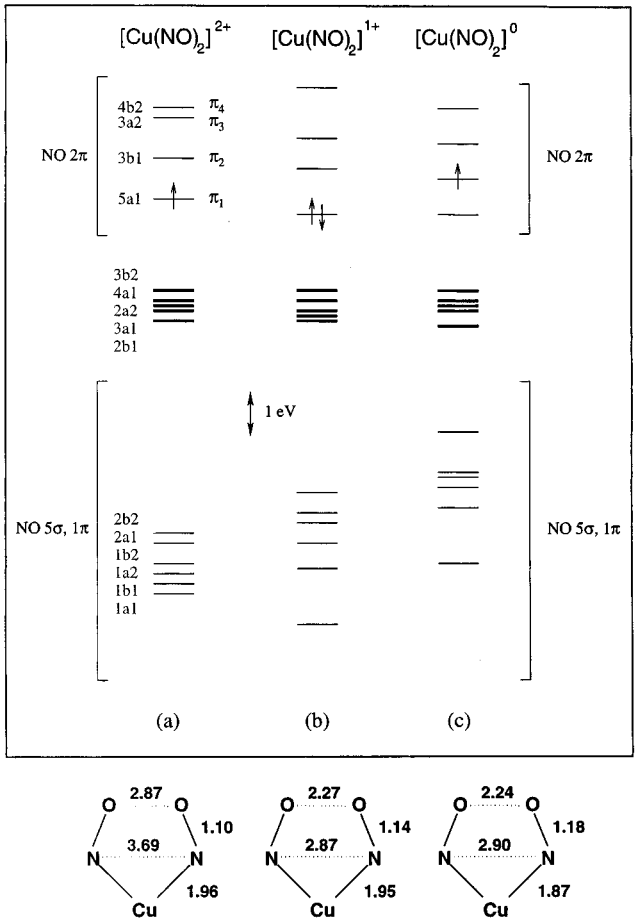

Figure 3. Molecular orbital diagrams for N-down dinitrosyl binding to bare Cu^{2+} (a), Cu^{+} (b), and Cu^{0} (c). For ease of interpretation, the orbitals are shifted vertically so that the top of the Cu d orbital manifolds have the same energy. Levels below those indicated by arrows are all doubly occupied, those above are empty, and those with a dominant Cu d component are indicated by bold lines.

The inclusion of additional oxygen coordination (as water ligands) at the Cu center does not alter this qualitative description of NO binding to Cu^{2+}. The water ligands donate additional charge to the Cu^{2+} center, decreasing somewhat its ability to accept electron density from the NO ligands, and the water-based levels mix with the Cu-based d levels, but the characterization as $[(H_2O)_xCu(I)-(NO)_2^{+}]$ remains accurate. The NO bond lengths increase slightly with increasing coordination, reflecting the decreasing reducibility of the Cu center. The additional coordination also forces the two NO ligands closer together, decreasing both the N−N and O−O separations and the N−Cu−N angle. Further, the first and second NO binding energies decrease monotonically with increasing Cu coordination (Table 3).

TABLE 3: Successive BP86 N-Down NO Binding Energies and Isomerization Energies to O-Down Dinitrosyl and Hyponitrite Structures, in kcal mol^{-1}

	+1st NO[a]	+2nd NO[b]	ΔE^c_{O-down}	ΔE^d_{hypo}
		Cu^{2+} Systems		
Cu^{2+}	−159	−63		
$Cu(H_2O)^{2+}$	−99	−44		
$Cu(H_2O)_2^{2+}$	−73	−29		
$Cu(H_2O)_4^{2+}$	−35	−19		
		Cu^{+} Systems		
Cu^{+}	−35	−34	+19	+44
$Cu(H_2O)^{+}$	−35	−25	+17	+33
$Cu(H_2O)_2^{+}$	−15	−23	+17	+31
$Cu(H_2O)_4^{+}$	−16	−18	+16	+19
		Cu^{0} Systems		
Cu	−27	−33		+6
$Cu(H_2O)$	−37	−31		−5
$Cu(H_2O)_2$	−35	−35		−5
$Cu(H_2O)_4$	−41	−37		−21

[a] Energy of reaction $[Cu(H_2O)_x]^{n+} + NO \rightarrow [Cu(H_2O)_xNO]^{n+}$; also see ref 63. [b] Energy of reaction $[Cu(H_2O)_x(NO)]^{n+} + NO \rightarrow [Cu(H_2O)_x(NO)_2]^{n+}$. [c] Energy difference between $^1A_1$ $[Cu(H_2O)_x(ON)_2]^{+}$ and $^1A_1$ $[Cu(H_2O)_x(NO)_2]^{+}$. [d] Energy difference between $^3A_2$ $[Cu(H_2O)_xO_2N_2]^{n+}$ and $^1A_1$ $[Cu(H_2O)_x(NO)_2]^{n+}$.

The reduction of Cu^{2+} by NO has interesting implications for the successive binding energies of two NO ligands. As seen in Table 3, regardless of coordination, the first NO binds to $[Cu(H_2O)_x]^{2+}$ (column 2) much more strongly than the second (column 3), due to significantly different electrostatic attractions: the first NO binds to a formally Cu^{2+} center, while the

TABLE 4: Selected LSDA Geometric Parameters and BP86 Relative Energies for Cu^+-Bound N-Down Dinitrosyl and O-Down Dinitrosyl and Hyponitrite Species for Model 1], Constrained to C_s Symmetry: Bond Lengths in Å, Bond Angles in Degrees, and Energies in kcal mol^{-1}

species	state	Cu−A[a]	N−N	N−O	Cu−O_H	A−Cu−A[a]	Cu−A−B[a,b]	*E*[c]
$[Al(OH)_4Cu(NO)_2]$	$^1A'$[d]	1.866	2.604	1.165	1.956	88.2	126.4	
		1.875		1.162			126.1	
$[Al(OH)_4Cu(ON)_2]$	$^1A'$[d]	1.996	1.772	1.188	1.940	75.1	126.3	18
		1.999		1.185			126.3	
$[Al(OH)_4CuO_2N_2]$	$^3A''$[e]	1.882	1.239	1.301	1.943	79.6	113.6	17
		1.912		1.299			112.3	

[a] A = N for N-down complexes; A = O for O-down complexes. [b] B = O for N-down complexes; B = N for O-down complexes. [c] Energy relative to $[Al(OH)_4Cu(NO)_2]$. [d] Correlates to $^1A_1$ under C_{2v} symmetry. [e] Correlates to $^1A_2$ under C_{2v} symmetry.

second binds to effectively a Cu^+ ion. Previous work has demonstrated stronger NO binding to Cu^{2+} than to Cu^+.[36,37] The large disparity in first and second NO binding energies may in part account for the lack of experimental evidence for Cu^{2+}−dinitrosyls in Cu-exchanged zeolites. In addition, the preference for high coordination to the lattice and/or extralattice ions may prevent two NO from coordinating to a zeolite-bound Cu^{2+}.

$[Cu(H_2O)_x(NO)_2]^+$. Both linear and bent conformations of $[Cu(NO)_2]^+$ exist, the former a triplet ($^3\Sigma_g^-$) and the latter a singlet ($^1A_1$), with a negligible difference in energy between the two (Table 2). As with bent $[Cu(NO)_2]^{2+}$, the O−O separation is less than the N−N separation in bent $[Cu(NO)_2]^+$, but the N−O separation (1.141 Å) is close to that in free NO (1.15 Å) and $[CuNO]^+$ (1.137 Å).[36] Figure 3b shows the molecular orbital diagram for bent $[Cu(NO)_2]^+$ ($^1A_1$). Its electronic structure is derived from $[Cu(NO)_2]^{2+}$ by the addition of an electron to the singly occupied NO 2π manifold in a spin-paired (resulting in the singlet state shown in Figure 3) or in a spin-aligned fashion. Here again, the ordering of the NO-derived levels is identical to that of the free NO dimer. The bonding situation in $[Cu(NO)_2]^+$ can thus be described as $[Cu(I)-^{1,3}(NO)_2]$; that is, no net electron transfer occurs between the Cu^+ ion and the pair of nitrosyl ligands. Inclusion of additional water coordination does not alter this qualitative picture, but only introduces relatively minor perturbations on the N−O, N−N, and O−O separations.

As shown in Table 3, the first and second binding energies of NO to Cu^+ are very similar, but decrease slightly with increasing Cu coordination. The first NO binding leaves the oxidation state of Cu unchanged, so that the second NO interacts with a Cu in approximately the same oxidation state. The second NO might be expected to have a lower binding energy than the first because of the tendency of Cu^+ to low coordination,[36] but the favorable interaction between the pair of nitrosyl ligands apparently offsets this effect. Slight differences do arise due to particular preferences in geometries; for instance, the preference of Cu^+ for tetrahedral coordination makes the second NO binding energy to $[Cu(H_2O)_2]^+$ greater than the first. The similarity in first and second NO binding energies to Cu^+ is consistent with the ready generation of dinitrosyl species on Cu^+ sites in Cu-exchanged zeolites.

We have recently reported calculated symmetric and antisymmetric NO stretching frequencies for Cu^+−dinitrosyl species,[38] using the same models as those considered here. The results are in good agreement with the observed infrared spectrum of these species in Cu-exchanged zeolites.[9−11,13−17] Estimates of the N−Cu−N angle based on vibrational frequency measurements yield a value of 104° if the integrated intensities are used and 90° if the peak intensities are used.[17] Our calculations consistently yield a value of about 90° in all complexes with at least one water ligand, in agreement with the latter experimental estimate.

The general geometric features that we find for the Cu^+-dinitrosyl complexes (specifically, a planar structure, with NO ligands tilted inward) differ qualitatively from a number of earlier descriptions. Moser[2] speculated that the N ends of two N-down nitrosyls would tend to pair up, perhaps with one NO ligand bound linearly and the other bent; we find no evidence for such a binding mode. Larger cluster calculations on two-coordinated Cu^+ sites have recently been reported by two groups.[42,43] Yokomichi *et al.*[42] appear to have constrained the NO ligands in a *trans*-like structure, which we do not find to be a favorable binding mode. Trout *et al.*[43] find that the Cu−N−O angle is always very nearly 180° in both mono- and dinitrosyl complexes, in direct opposition with our results. The NO vibrational frequencies obtained in these earlier studies are in poor agreement with experiment. In order to demonstrate the robustness of our results with respect to the Cu coordination environment, we have performed calculations on Cu^+−dinitrosyl complexes using a zeolite model similar to those in refs 42 and 43 (**1**) and report structural results for this model in Table 4.

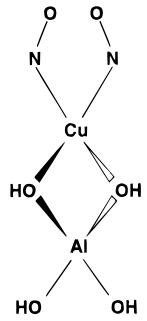

1

The ligand geometry predicted using this larger model agrees nearly quantitatively with the two-water-ligand model results. Further, LSDA dinitrosyl vibrational frequencies calculated with the larger model (1717, 1844 cm^{-1}) are in excellent agreement with experiment.[9−17,38] The structural features reported here—in particular, the preference of NO ligands for bending toward one another—are robust with respect to the choice of zeolite model.

$[Cu(H_2O)_x(NO)_2]$. Isolated uncharged Cu atoms are not anticipated to be found in zeolites. For completeness, however, we consider NO binding to bare and water-ligated Cu(0). Linear N−Cu−N ($^2\Pi_u$) and bent N−Cu−N ($^2B_1$) $[Cu(NO)_2]$ structures are found to be nearly identical in energy. The N−O bond length in the bent structure (1.184 Å) is greater than that in free NO (1.15 Å). As shown in Figure 3c, the electronic structure of $[Cu(NO)_2]$ is derived from that of $[Cu(NO)_2]^+$ by the addition of another electron into the NO 2π manifold, reflecting an effective transfer of electronic charge from Cu to the NO ligands, which manifests itself in increased N−O bond lengths. The bonding situation can thus be represented as $[Cu(I)-(NO)_2^-]$. Increasing the coordination of Cu does not alter

TABLE 5: Selected LSDA Geometric Parameters, Cu d Population, and BP86 Fragmentation Energies for $[Cu(H_2O)_x(ON)_2]^+$ and $[Cu(H_2O)_xO_2N_2]^{n+}$ Complexes: Bond Lengths in Å, Bond Angles in Degrees, and Energies in kcal mol^{-1}

	state	Cu−O_N	N−O	N−N	Cu−O_H	O−Cu−O	Cu−O−N	Cu d pop.	E^a
					$[Cu(H_2O)_x(ON)_2]^+$				
$x=0$	$^1A_1$	2.060	1.153	2.010		80.4	123.5	9.83	−49.4
$x=1$	$^1A_1$	2.043	1.159	1.965	1.907	77.0	127.0	9.75	−83.1
$x=2$	$^1A_1$	2.034	1.168	1.902	2.009	75.5	127.6	9.71	−101.9
$x=4$	$^1A_1$	2.093	1.170	1.916	2.166	72.4	130.1	9.78	−114.3
$x=0$	$^3B_1$	2.056	1.160	1.964		80.9	121.9	9.87	−42.2
$x=1$	$^3B_1$	1.986	1.164	1.962	1.986	80.0	125.6	9.78	−76.7
$x=2$	$^3B_1$	2.169	1.176	1.778	1.924	74.4	121.8	9.72	−100.7
$x=4$	$^3B_1$	2.254	1.179	1.755	2.126	71.0	124.8	9.78	−113.8
					$[Cu(H_2O)_xO_2N_2]^+$				
$x=0$	$^1A_1^*$	1.927	1.270	1.161		82.5	105.9	9.57	−18.4
$x=1$	$^1A_1^*$	1.875	1.286	1.170	1.882	80.1	109.9	9.45	−62.7
$x=2$	$^1A_1^*$	1.900	1.285	1.170	2.063	80.6	109.6	9.49	−78.4
$x=4$	$^1A_1^*$	1.894	1.308	1.182	2.161	80.9	110.4	9.46	−108.7
$x=0$	$^3A_2$	1.953	1.255	1.259		79.1	100.3	9.61	−24.4
$x=1$	$^3A_2$	1.924	1.263	1.266	1.896	78.3	113.4	9.51	−66.5
$x=2$	$^3A_2$	1.928	1.276	1.242	2.011	78.3	113.0	9.48	−87.9
$x=4$	$^3A_2$	1.940	1.284	1.261	2.167	76.5	114.3	9.49	−110.7
					$[Cu(H_2O)_xO_2N_2]$				
$x=0$	$^2B_2$	1.883	1.319	1.215		85.8	106.4	9.65	−53.5
$x=1$	$^2B_2$	1.871	1.329	1.216	1.938	83.3	109.8	9.58	−74.8
$x=2$	$^2B_2$	1.886	1.333	1.218	2.146	83.3	109.5	9.62	−81.1
$x=4$	$^2B_2$	1.958	1.348	1.221	2.247	79.5	111.9	9.61	−97.5

[a] Energy of reaction $Cu^{n+} + xH_2O + 2NO \rightarrow [Cu(H_2O)_x(ON)_2]^+$ or $[Cu(H_2O)_xO_2N_2]^{n+}$.

this description. Table 3 contains the successive binding energies of the first and second nitrosyl ligands to bare and water-ligated Cu(0). The second NO binds more strongly to Cu than the first; the first NO binds to a neutral Cu, while the second binds to effectively a Cu^+ center. The first and second NO binding energies do increase slightly as the Cu coordination increases, *i.e.*, as the Cu center becomes a better electron donor.

B. O-Down Structures. NO can also bind to Cu^{n+} centers through its O atom. Stable O-down mononitrosyl complexes exist for Cu^0 and Cu^+ with 0−4 water ligands and for highly coordinated Cu^{2+}. In each case, the O-down complex is less stable than the corresponding N-down complex by 10−15 kcal mol^{-1}. The geometric and electronic structures of the O-down complexes are similar to that of the N-down variety, with N−O separations slightly longer in the O-down complexes. For both orientations, bent binding of NO is preferred to linear binding in neutral and 1+ cases by about 10−15 kcal mol^{-1}.

Although the addition of a second NO ligand is not expected to change this preference for N-down binding, it is useful to consider possible O-down structures, as such less stable species may in fact play a greater role in NO decomposition (cf. section VI). O-down chelating and bridging transition metal hyponitrite complexes are known to exist.[69] Copper hyponitrites have been observed[70,71] but have not been structurally characterized; platinum hyponitrites have been shown to have an O-down bidendate structure with a relatively short N−N bond (≈1.21 Å).[62]

Two distinct types of O-down dinitrosyl complexes are found within the water−ligand model. The first, which we denote $[Cu(H_2O)_x(ON)_2]^{n+}$, are similar in geometric and electronic structure to the N-down complexes just discussed: the N−O separations are small, and the two NO tilt inward, so that the N−N separation is less than the O−O separation. The second, which we denote $[Cu(H_2O)_xO_2N_2]^{n+}$, are more closely akin to the anionic hyponitrites discussed in section III than to a dinitrosyl species: the N−N separation is considerably reduced and the N−O separations increased compared to both N-down and O-down dinitrosyl complexes. Neither of these binding modes is stable to dissociation on Cu^{2+}; we focus here on the Cu^+ and Cu^0 complexes.

$[Cu(H_2O)_x(ON)_2]^+$ and $[Cu(H_2O)_xO_2N_2]^+$. Both dinitrosyl (with N−N separations of ≈1.9−2.0 Å) and hyponitrite (with N−N separations of ≈1.2 Å) binding modes exist, and for each type both singlet and triplet states are accessible. The important structural parameters, Cu d populations, and BP86 binding energies are summarized in Table 5. The singlet dinitrosyl states, although of the same symmetry, are electronically distinct from the singlet hyponitrite ones; the former are labeled $^1A_1$ and the latter $^1A_1^*$ in Table 5 to highlight this difference.

The electronic structure of $[Cu(ON)_2]^+$ ($^1A_1$, Figure 4a) is similar to that of the N-down isomer, $[Cu(NO)_2]^+$ (Figure 3b); the ordering of the NO-derived levels is preserved and is identical to that of free $(NO)_2$. The bonding situation in this and the water-coordinated homologues can thus be represented as $[(H_2O)_xCu(I)-(ON)_2]$, with little effective charge transfer between the Cu and $(ON)_2$ fragments. The Cu d populations (Table 5) are consistent with this representation and are in fact even larger than the corresponding N-down populations (Table 2). The singlet states are again slightly more stable than the triplet, although the separation is small and decreases with increasing Cu coordination. Increasing coordination also drives a decrease in N−N separation to a value less than that in the free NO dimer and with the separation in the triplet states less than in the singlet states.

The electronic structure of $[CuO_2N_2]^+$ (Figure 4b) is qualitatively different from the N-down and O-down dinitrosyls considered thus far. The Cu d and NO derived levels are strongly mixed, making assignment of the Cu oxidation state more difficult. Both the Cu d populations (Table 5) and decomposition of the molecular orbitals indicate an oxidation state closer to Cu(II) than to Cu(I). Comparison of the molecular orbital diagrams in Figure 2 with that of $[CuO_2N_2]^+$ indicates a similarity to an $N_2O_2^-$ anion; a decomposition in terms of fragment molecular orbitals reinforces this separation into Cu^{2+} and $N_2O_2^-$ fragments, with mixing occuring almost exclusively between the b_2 Cu d orbital and the $1b_2$ and $2b_2$ levels of $N_2O_2^-$ (Figure 2). The bonding situation can thus be characterized as $[Cu(II)-(O_2N_2)^-]$. Electron transfer from Cu to the NO ligands drives formation of the hyponitrite structure and thereby of a short N−N bond. This metal-mediated N−N

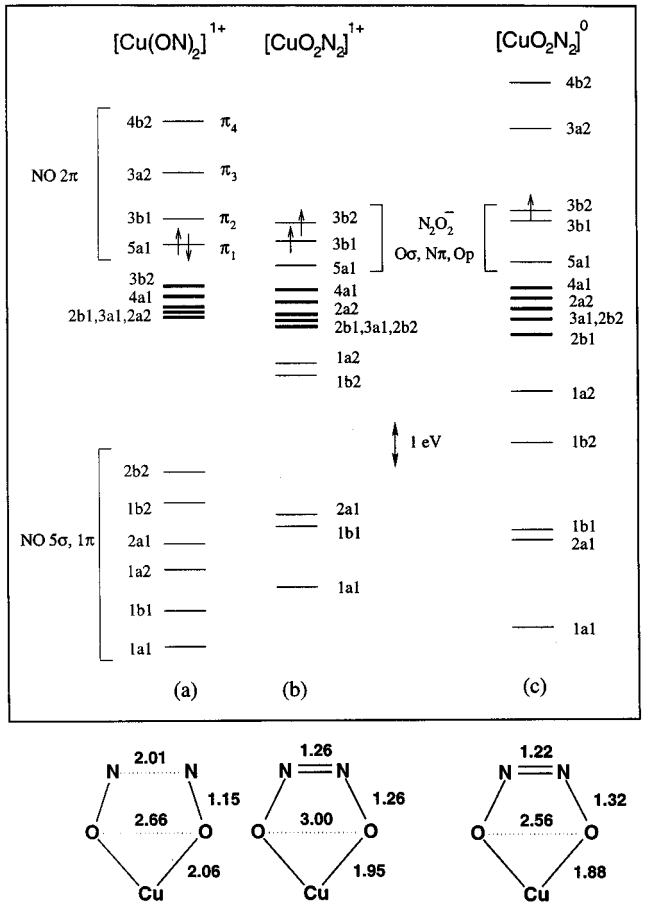

Figure 4. Molecular orbital diagrams for O-down dinitrosyl binding to bare Cu^+ (a), hyponitrite-like binding to bare Cu^+ (b), and hyponitrite-like binding to bare Cu^0 (c). For ease of interpretation, the orbitals are shifted vertically so that the top of the Cu d orbital manifolds have the same energy. Levels below those indicated by arrows are all doubly occupied, those above are empty, and those with a dominant Cu d component are indicated by bold lines.

bond formation suggests a possible role for Cu^+ in catalyzing NO decomposition.

Inclusion of water ligands does not alter this qualitative bonding picture, nor does it significantly alter the hyponitrite geometry, although it does modify the relative energies of various binding modes, by increasing the electron density at the Cu^+ center. As shown in the fourth column of Table 3, the singlet N-down dinitrosyl structure is more stable than the singlet O-down form by approximately 20 kcal mol^{-1}, regardless of coordination. The triplet hyponitrite structure is much less favorable at low coordination; as the Cu coordination (and electron-donating ability) increases, the hyponitrite form becomes increasingly favorable (Table 3, column 5). In fact, using the explicit Al-containing zeolite model introduced earlier (**1**), the same O-down binding modes are observed (Table 4), but with the hyponitrite slightly lower in energy than the dinitrosyl complex. While the Cu^+-hyponitrites may not be stable enough to be observed experimentally in Cu−zeolites, they may play an important role in N−N bond forming processes in these materials.

$[Cu(H_2O)_xO_2N_2]$. A neutral Cu atom is a much stronger electron donor than a Cu^+ ion; consequently, the only stable O-down structure in this case is the hyponitrite. In fact, with the exception of the bare Cu atom, the hyponitrites are more stable than the N-down dinitrosyl complexes (last column of Table 3). The electronic structure of $[CuO_2N_2]$ (Figure 4c) is closely related to the monocation, and charge and orbital

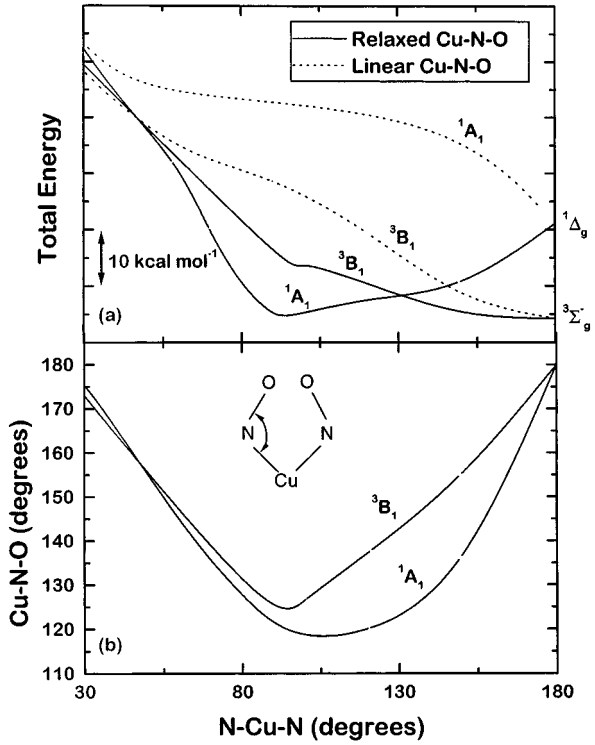

Figure 5. (a) Variation of total BP86 energy of $[Cu(NO)_2]^+$ as a function of N−Cu−N angle for both linearly constrained and relaxed Cu−N−O angle. (b) Corresponding variation of relaxed Cu−N−O angle. All other geometric parameters are optimized.

analyses are consistent with the description $[(H_2O)_xCu(I)-O_2N_2^-]$. Unlike the dinitrosyl complexes, the hyponitrites do bind water ligands strongly (last column in Table 5), as a result of the Cu oxidation. The geometries of the neutral hyponitrites are similar to the Cu^+ hyponitrites, with some modifications associated with the greater electron donation of Cu(0). The structures $[Cu(H_2O)_xO_2N_2]$ are typical of metal hyponitrites.[50]

V. Coupling between Nitrosyl Ligands in Cu−Dinitrosyl Complexes

As noted above, a feature common to all the Cu−dinitrosyl complexes is the "leaning inward" of the nitrosyl ligands, suggesting some electronic interaction between the ligands, but mediated through the atoms not directly bound to the Cu center. In this section, we further interrogate the origins of this structure, focusing on $[Cu(NO)_2]^+$ as a prototype.

A single NO binds to a Cu^+ ion in a bent fashion, both to minimize overlap between the filled Cu d and partially filled NO 2π orbitals and to allow mixing of the partially filled 2π and vacant Cu 4s.[36] A second NO can bind to Cu in a spin-paired or spin-aligned manner. The global minimum of $[Cu(NO)_2]^+$ is a completely linear ($D_{\infty h}$) $^3\Sigma_g^-$ structure, in which the two unpaired electrons are delocalized in π_u orbitals extending across the whole molecule. Pairing both electrons in one of the π_u orbitals produces a singlet state ($^1\Delta_u$) 16 kcal mol^{-1} higher in energy. As shown in Figure 5a, if the N−Cu−N angle is varied while the NO are constrained to remain linear, both singlet and triplet states rise monotonically in energy. In contrast, if the Cu−N−O angles are allowed to relax inward while varying the N−Cu−N coordinate and keeping the entire system planar, both states are stabilized, and in particular, a $^1A_1$ minimum energy structure is obtained. This stabilization occurs only if the ligands bend toward one another; bending only one ligand, or bending away from each other, does not lead to the same stabilization.

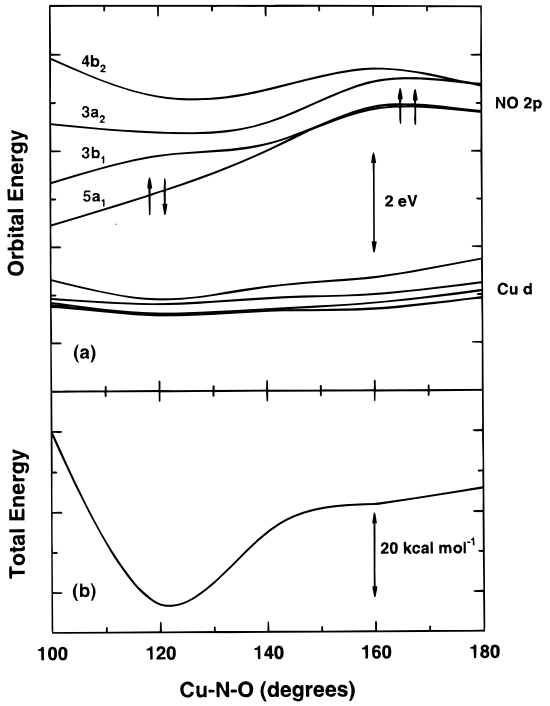

Figure 6. Evolution of BP86 energy levels (a) and BP86 total energy (b) of $[Cu(NO)_2]^+$ as a function of the Cu−N−O angle. The Cu−N bond length, N−Cu−N angle, and N−Cu−N−O dihedral angle are fixed at 1.95 Å, 95°, and 0°, respectively (corresponding to a N−N bond length of 2.87 Å), and the N−O bond length is optimized for a range of Cu−N−O angles.

A subtle interplay of metal−ligand and ligand−ligand interactions combine to produce the equilibrium dinitrosyl geometry. The molecular orbital diagram for $[Cu(NO)_2]^+$ is shown in the center of Figure 3 and is highly reminiscent of that for the NO dimer (Figure 2). For a qualitative understanding of the final structure, it is sufficient to focus on the two highest lying occupied orbitals: the NO-based $5a_1$ (**2**) and the Cu d-based $3b_2$ (**3**).

2 **3**

The $3b_2$ level is representative of the antisymmetric metal-ligand σ -bonding interaction, which helps bind the NO ligands to Cu but tends to force the ligands away from each other, because of its ligand−ligand antibonding character. In contrast, the $5a_1$ level is bonding both between the Cu and NO and between the two NO and thus tends to draw the NO together. A balance is achieved at an N−Cu−N angle of approximately 90° and an O−O separation of about 2.2 Å. Figure 6 shows the change in orbital and total energies for fixed (equilibrium) Cu−N separation and N−Cu−N angle, for a range of values of the Cu−N−O angle. Bending inward of the NO ligands is accompanied by a stabilization of the $5a_1$ level and decrease in the total energy by approximately 25 kcal mol^{-1} (Figure 6b). This equilibrium geometry is essentially constant with respect to additional coordination for a given Cu oxidation state (Table 2). Oxidation or reduction of $[Cu(NO)_2]^+$ by one electron only alters the occupation of the NO 2π -derived orbitals ($5a_1$ and $3b_1$) and diminishes or enhances the ligand−ligand coupling, respectively.

Similar orbital arguments hold in the case of the O-down dinitrosyls, with the roles of the N and O centers reversed. The ligand−ligand interactions—now mediated through the N centers—are increased compared to the N-down analogs, because of the larger N contribution to the 2π levels. The metal−ligand interactions are similarly decreased, producing a net destabilization compared to the N-down complexes.

It is interesting to contrast the Cu−dinitrosyl with Cu−dicarbonyl complexes, in which the 2π levels are vacant and ligand−ligand coupling is weak or nonexistent.[38] CO ligands are found to always bind linearly to a Cu cation, with the C−Cu−C angle in a dicarbonyl complex determined primarily by interligand repulsions and always greater than the N−Cu−N angle in the corresponding dinitrosyl complex. Further, the splitting between symmetric and antisymmetric C−O stretching modes is considerably less than the splitting between the corresponding N−O modes.[38]

The strong ligand−ligand interactions and similarity in electronic structure between free $(NO)_2$ and dinitrosyl complexes suggest that it may be appropriate to view $(NO)_2$ as a single, bidentate ligand. Evidence does exist for the enhanced dimerization of NO within zeolite nanopores.[74] It is possible that $(NO)_2$ may adsorb directly onto a Cu site in either the N-down or O-down orientation, with charge transfers from and to the ligand depending on the Cu oxidation state.

VI. NO Decomposition and N−N Bond Formation

A. Free NO Decomposition. We now attempt to assess the likelihood of participation of the dinitrosyl complexes in NO decomposition. We begin by considering the decomposition of free NO (reaction 1) by a concerted process in which two NO molecules pass through a symmetric-*cis* form of $(NO)_2$, simultaneously forming N−N and O−O bonds and breaking N−O bonds. The decomposition reaction 1 is exothermic by about 44 kcal mol^{-1} at the BP86 level of theory, in good agreement with the value of 43 kcal mol^{-1} determined from experimental atomization energies.[61,75] Figure 7 shows a schematic orbital correlation diagram[76−78] along such a pathway, including the evolution of 1π, 5σ, 2π, and 6σ derived levels of two isolated NO molecules (left), *cis*-$(NO)_2$ (middle), and N_2 and O_2 (right), with C_{2v} symmetry maintained throughout. Each of the three sets of molecules has a triplet ground state; the unpaired electrons are indicated by arrows in Figure 7. The occupied orbitals of two NO correlate with those of $(NO)_2$, and thus NO dimerization is symmetry allowed. The further decomposition to N_2 and O_2 is clearly symmetry forbidden: among majority spin levels, occupied (5σ) and vacant (6σ) levels of NO correlate, respectively, with vacant (2π) and occupied (1π) levels of N_2 and O_2 ; additional forbidden crossings occur among the minority spin levels. It follows that a major reorganization of charge density is necessary to decompose $(NO)_2$ to N_2 and O_2 and that the direct decomposition reaction will have a large energy barrier. The *formal* symmetry forbidden nature disappears when the molecular symmetry is relaxed (to C_s, for instance), but its effects will persist in the form of a large energy barrier.

An alternative argument can be made based on state correlations (Figure 8). The ground state of two isolated NO molecules and of the decomposition products is $^3B_1$, but the dominant configuration of the latter state ($a_2 \times b_2$) differs by a quadruple excitation from the leading configuration of the former ($a_1 \times b_1$).[79] Because the states are of the same total symmetry, they can mix along the reaction coordinate, allowing the entire reaction to proceed on the ground-state potential energy surface and avoiding the intended orbital crossing. Nevertheless, the

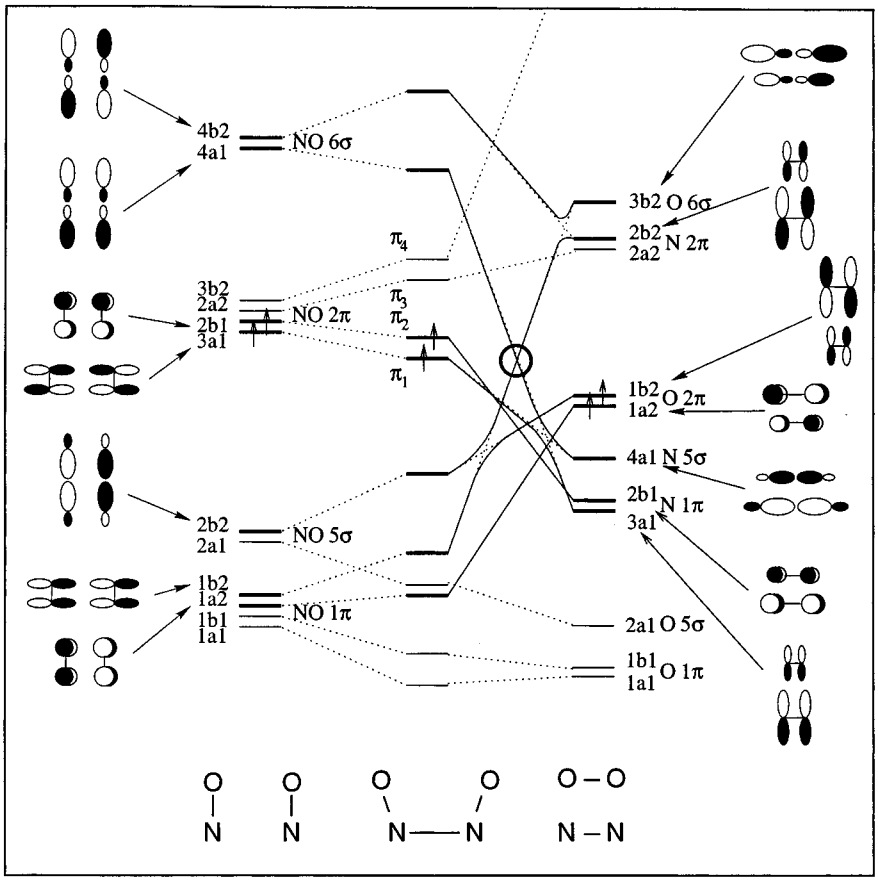

Figure 7. Orbital correlation diagram for two isolated NO molecules (left), the *cis*-symmetric dimer $(NO)_2$ (center), and N_2 and O_2 (right). Levels below those indicated by arrows are all doubly occupied, and those above are empty. Levels involved in forbidden crossings are connected by solid lines, and the levels themselves are darkened and pictured. The majority spin level crossing is indicated by a circle.

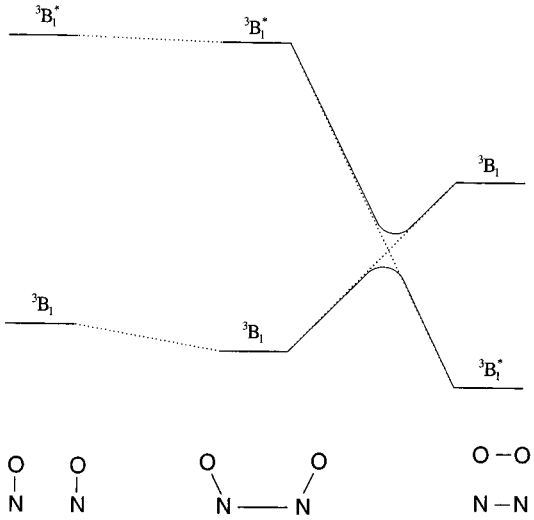

Figure 8. State correlation diagram for two isolated NO molecules (left), the *cis*-symmetric dimer $(NO)_2$ (center), and N_2 and O_2 (right).

presense of an underlying orbital crossing, and the expected large difference in energy between the ground and quadruply excited states, implies that the reaction barrier will be large.

B. NO Decomposition and N−N Bond Formation on Zeolite-Bound Cu Ions. The preceeding results make clear the origin of the large barrier to direct decomposition of NO. As we have seen above, the character and ordering of the NO-derived levels in Cu-bound dinitrosyl complexes (either $[Cu(NO)_2]^{n+}$ or $[Cu(ON)_2]^{n+}$) are essentially unchanged from those shown in Figure 7 for two isolated NO molecules or for free $(NO)_2$. The only modification introduced by the Cu center is an increase or decrease by one electron of the occupancy of the 2π levels with variation in the formal Cu oxidation state. The direct decomposition of any of these complexes to produce N_2 and O_2 (reaction 2) is thus forbidden by orbital symmetry in the same way that the free decomposition reaction is. Reaction 2 is expected to have an energy barrier at least as large as that of the free decomposition reaction (because Cu coordination stabilizes the reactants but not the products) and is not an important reaction pathway for Cu−dinitrosyl complexes in Cu-exchanged zeolites.

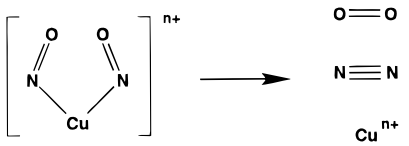

(2)

A number of workers have considered short N−N bond-containing structures, **3**, for N-down transition metal dinitrosyl complexes with d electron counts lower than the Cu systems studied here. Kersting and Hoffmann[80] used extended Hückel orbital and total energies to investigate $ReCl_4(NO)_2^-$, which has a $\{Re(NO)_2\}^6$ core, but found that N−N bond formation was not energetically favorable. Casewit and Rappé[81] used *ab initio* (GVB-CI) methods to support a short N−N bond structure in $FeCl_2(H_2O)_2(NO)_2$, which has a $\{Fe(NO)_2\}^8$ core. Formation of a N-down hyponitrite structure with a short N−N bond from adsorbed dinitrosyl species has also been suggested to occur on Rh surfaces,[3] and Moser[2] long ago proposed such a structure (**4**) for Cu dinitrosyl species.

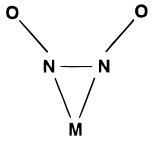

4

None of the N-down dinitrosyl results presented in section IV suggest this type of N−N coupling. Decreasing the N−Cu−N angle in $[Cu(NO)_2]^+$ below its equilibrium value while relaxing all other geometric parameters (Figure 5a) leads to dissociation into Cu^+ and $^1A_1$ or $^3B_1$ $(NO)_2$ fragments rather than N−N bond formation. If instead of varying the N−Cu−N angle, the N−N separation is artificially decreased, the energy of the system again rapidly increases, and an initially vacant out-of-plane bonding combination of NO 2π orbitals is stabilized below one of the Cu d levels, reflecting an approximate one-electron oxidation of the Cu center. The resultant electronic state is reminiscent of the "hyponitrite-like" O-down structures discussed earlier, and in fact geometric relaxation of this configuration does return the system to an O-down structure. In a similar fashion, we find no evidence for N−N coupling in the $[Cu(NO)_2]$ or $[Cu(NO)_2]^{2+}$ systems.

We conclude then that the stable Cu dinitrosyl complexes identified in experimental investigations do not contain an N−N bond, nor are they precursors to the formation of N−N bond-containing products: they are likely spectators and not participants in NO decomposition. The only structures identified in this study that do suggest the forming of a new N−N bond on a Cu cation are the hyponitrites, $[Cu(O_2N_2)]^+$. Because of the difference in electron configurations, it is unlikely that the metastable hyponitrite structure can be formed directly from either an N-down or O-down dinitrosyl. More likely, if they exist, the hyponitrites are formed by the sequential addition of two NO in an O-down fashion on a single Cu^+ center. Although their stability is enhanced by increasing electron density at the Cu center (for instance, by high Cu coordination or proximity to a strong Lewis base site), the hyponitrites may exist only transiently in zeolites, making their experimental identification difficult.

It is easy to verify that decomposition of the hyponitrite complexes to N_2 and O_2 is symmetry forbidden, and we conclude that an NO decomposition mechanism based on a single-step disproportionation of Cu-bound dinitrosyl or hyponitrite-like species to free N_2 and O_2 is highly unlikely. NO decomposition on a single Cu site, if it occurs at all, must occur in a multistep process, for instance, by the formation of a N_2O intermediate.[10,13,16,17] The N−N bond forming step in such a mechanism is unlikely to involve dinitrosyl (N-down and O-down) complexes; however, the hyponitrite-like complexes identified here hold considerable promise as precursors for such a multi-step decomposition process.[82]

VII. Summary and Conclusions

We have used simple cluster models to examine Cu−dinitrosyl complexes in zeolites and to address the question of N−N bond formation on a Cu center. Our main conclusions can be summarized as follows.

1. N-down binding is the preferred binding mode for two NO ligands to Cu^{2+} or Cu^+. The NO ligands adopt a tilted conformation, in which the N−N separation is larger (≈2.8 Å) than the O−O separation. Electron transfer maintains the Cu in an effective Cu(I) oxidation state, with binding on Cu^{2+} and Cu^+ represented as $[Cu(I)-(NO)_2^+]$ and $[Cu(I)-(NO)_2]$, respectively.

2. Two different metastable O-down binding modes are observed on Cu^+, but not on Cu^{2+}. The first is similar in structure to the N-down dinitrosyl complex, with the N and O atoms reversed in position and some additional coupling between the N centers (N−N bond length ≈ 2 Å); it can be described as $[Cu(I)-(ON)_2]$. The second is a Cu-bound hyponitrite, formed by electron transfer from Cu^+ to the two NO and having a short N−N bond (N−N bond length ≈ 1.2 Å); it is characterized as $[Cu(II)-O_2N_2^-]$. Both N- and O-down dinitrosyls are more stable than the hyponitrites, but the energy difference decreases with increasing Cu coordination.

3. A Cu ion does support the coupling between two bound NO ligands, but the primary interaction occurs through the atoms not directly coordinated to Cu, *i.e.*, through the O centers in N-down systems and through the N centers in O-down systems. True N−N bond formation occurs only in the hyponitrites.

4. The symmetry-forbidden nature of the direct decomposition of NO to N_2 and O_2 is not altered by NO binding to Cu, regardless of Cu oxidation state, and this mechanism is unlikely to account for the NO decomposition activity of Cu-exchanged zeolites. Cu^+ centers can promote the formation of N−N bonds via Cu−hyponitrites; these complexes may participate in more complex multistep NO decomposition processes. Such processes are currently under investigation in our laboratories.[82]

Acknowledgment. R.R. and J.B.A. would like to acknowledge support by NSF under Grant No. NSF-1-5-30897 (8), the National Center for Supercomputing Applications (NCSA), the Cornell Theory Center (CTC), and three summer appointments for R.R. at the Ford Research Laboratory.

References and Notes

(1) Shelef, M.; Kummer, J. T. *Chem. Eng. Prog. Symp. Ser.* **1971**, *67*, 74.
(2) Moser, W. R. *The Catalytic Chemistry of Nitrogen Oxides*; Klimisch, R. L., Larson, J. G., Eds.; Plenum: New York, 1975; p 33.
(3) Ward, T. R.; Hoffmann, R.; Shelef, M. *Surf. Sci.* **1993**, *289*, 85.
(4) Koshi, M.; Asaba, T. *Int. J. Chem. Kinet.* **1979**, *11*, 305.
(5) Shelef, M. *Chem. Rev.* **1995**, *95*, 209.
(6) Centi, G.; Perathoner, S. *Appl. Catal. A* **1995**, *132*, 179.
(7) (a) Iwamoto, M.; Mizuno, N. *J. Automot. Eng. (Part D Proc. Inst. Mech. Eng.)* **1993**, *207*, 23. (b) Iwamoto, M.; Hamada, H. *Catal. Today* **1991**, *10*, 57.
(8) Jang, H.-J.; Hall, W. K.; d'Itri, J. L. *J. Phys. Chem.* **1996**, *100*, 9416.
(9) Hoost, T. E.; Lafromboise, K. A.; Otto, K. *Catal. Lett.* **1996**, *37*, 153.
(10) Cheung, T.; Bhargava, S. K.; Hobday, M.; Foger, K. *J. Catal.* **1996**, *158*, 301.
(11) Beutel, T.; Sárkány, J.; Lei, G.-D.; Yan, J. Y.; Sachtler, W. M. H. *J. Phys. Chem.* **1996**, *100*, 845.
(12) Yamashita, H.; Matsuoka, M.; Tsuji, K.; Shioya, Y.; Anpo, M. *J. Phys. Chem.* **1996**, *100*, 397.
(13) Aylor, A. W.; Larsen, S. C.; Reimer, J. A.; Bell, A. T. *J. Catal.* **1995**, *157*, 592.
(14) Dědeček, J.; Sobalík, Z.; Tvaružková, Z.; Kaucký, D.; Wichterlová, B. *J. Phys. Chem.* **1995**, *99*, 16327.
(15) Spoto, G.; Zecchina, A.; Bordiga, S.; Ricchiardi, G.; Martra, G. *Appl. Catal. B: Env.* **1994**, *3*, 151.
(16) Valyon, J.; Hall, W. K. *J. Phys. Chem.* **1993**, *97*, 1204.
(17) Giamello, E.; Murphy, D.; Magnacca, G.; Morterra, C.; Shioya, Y.; Nomura, T.; Anpo, M. *J. Catal.* **1992**, *136*, 510.
(18) Hoost, T. E.; Lafromboise, K. A.; Otto, K. *Catal. Lett.* **1995**, *33*, 105.
(19) Komatsu, T.; Ogawa, T.; Yashima, T. *J. Phys. Chem.* **1995**, *99*, 13053.
(20) Iwamoto, M.; Yahiro, H.; Mizuno, N.; Zhang, W. X.; Mine, Y.; Furukawa, H.; Kagawa, S. *J. Phys. Chem.* **1992**, *96*, 9360.
(21) Petunchi, J. O.; Marcelin, G.; Hall, W. K. *J. Phys. Chem.* **1992**, *96*, 9967.
(22) Anderson, M. W.; Kevan, L. *J. Phys. Chem.* **1987**, *91*, 4174.
(23) Kucherov, A. V.; Hubbard, C. P.; Shelef, M. *J. Catal.* **1995**, *157*, 603.

(24) Slinkin, A. A.; Kucherov, A. V.; Chuylkin, N. D.; Korsunov, V. A.; Klyachko, A. L.; Nikishenko, S. B. *Kinet. Katal.* **1990**, *31*, 698.
(25) Kucherov, A. V.; Slinkin, A. A. *J. Phys. Chem.* **1989**, *93*, 864.
(26) Kucherov, A. V.; Slinkin, A. A.; Kondrat'ev, D. A.; Bondarenko, T. N.; Rubinstein, A. M.; Minachev, Kh. M. *Zeolites* **1985**, *5*, 320.
(27) Larsen, S. C.; Aylor, A.; Bell, A. T.; Reimer, J. A. *J. Phys. Chem.* **1994**, *98*, 11533.
(28) Hamada, H.; Matsubayashi, N.; Shimada, H.; Kintaichi, Y.; Ito, T.; Nishijima, A. *Catal. Lett.* **1990**, *5*, 189.
(29) Liu, D.-J.; Robota, H. J. *Catal. Lett.* **1993**, *21*, 291.
(30) Liu, D.-J.; Robota, H. J. *Appl. Catal.* **1994**, *4*, 155.
(31) Grünert, W.; Hayes, N. W.; Joyner, R. W.; Shpiro, E. S.; Siddiqui, M. R.; Baeva, G. N. *J. Phys. Chem.* **1994**, *98*, 10832.
(32) Corbin, D. F.; Abrams, L.; Jones, G. A.; Eddy, M. M.; Harrison, W. T. A.; Stucky, G. D.; Cox, D. E. *J. Am. Chem. Soc.* **1990**, *112*, 4821.
(33) Kung, M. C.; Kung, H. H. *Catal. Rev.* **1985**, *27*, 425.
(34) Portella, L.; Grange, P.; Delmon, B. *Catal. Rev.-Sci. Eng.* **1995**, *37* (4), 699, and references therein.
(35) Zecchina, A.; Garrone, E.; Morterra, C.; Coluccia, S. *J. Phys. Chem.* **1975**, *79*, 978.
(36) Schneider, W. F.; Hass, K. C.; Ramprasad, R.; Adams, J. B. *J. Phys. Chem.* **1996**, *100*, 6032.
(37) Hass, K. C.; Schneider, W. F. *J. Phys. Chem.* **1996**, *100*, 92992.
(38) Ramprasad, R.; Schneider, W. F.; Hass, K. C.; Adams, J. B., *J. Phys. Chem. B* **1997**, *101*, 1940.
(39) Trout, B. L.; Chakraborty, A. K.; Bell, A. T. *J. Phys. Chem.* **1996**, *100*, 4173.
(40) Sauer, J.; Ugliengo, P.; Garrone, E.; Saunders, V. R. *Chem. Rev.* **1994**, *94*, 2095.
(41) Kyrlidis, A.; Cook, S. J.; Chakraborty, A. K.; Bell, A. T.; Theodorou, D. N. *J. Phys. Chem.* **1995**, *99*, 1505.
(42) Yokomichi, Y.; Yamabe, T.; Ohtsuka, H.; Kakumoto, T. *J. Phys. Chem.* **1996**, *100*, 14424.
(43) Trout, B. L.; Chakraborty, A. K.; Bell, A. T. *J. Phys. Chem.* **1996**, *100*, 17582.
(44) Baerends, E. J.; Ellis, D. E.; Ros, P. *Chem. Phys.* **1973**, *2*, 41.
(45) Vosko, S. H.; Wilk, L.; Nusair, M. *Can. J. Phys.* **1980**, *58*, 1200.
(46) Becke, A. D. *Phys. Rev. A* **1988**, *38*, 3098.
(47) Perdew, J. P. *Phys. Rev. B* **1986**, *33*, 8822.
(48) TeVelde, G.; Baerends, E. J. *J. Comput. Chem.* **1993**, *14*, 1347.
(49) Complete details of all structures are available directly from the authors.
(50) Laane, J.; Ohlsen, J. R. *Prog. Inorg. Chem.* **1980**, *27*, 465.
(51) Dinerman, C. E.; Ewing, G. E. *J. Chem. Phys* **1970**, *53*, 626.
(52) Kukolich, S. G. *J. Mol. Spectrosc.* **1983**, *98*, 80.
(53) Scott, R. L. *Mol. Phys.* **1966**, *11*, 399.
(54) Billingsley, J.; Callear, A. B. *Trans. Faraday Soc.* **1971**, *67*, 589.
(55) Stirling, A.; Pápai, I.; Mink, J.; Salahub, D. R. *J. Chem. Phys.* **1994**, *100*, 2910.
(56) Gonzalez-Luque, R.; Merchan, M.; Roos, B. O. *Theor. Chim. Acta* **1994**, *88*, 425.
(57) Lee, T. J.; Rendell, A. P.; Taylor, P. R. *J. Phys. Chem.* **1990**, *94*, 5463.
(58) Lee, T. J.; Rice, J. E.; Scuseria, G. E.; Schaefer, H. F. *Theor. Chim. Acta* **1989**, *75*, 81.
(59) McKee, M. L. *J. Am. Chem. Soc.* **1995**, *117*, 1629.
(60) Arnold, D. W.; Neumark, D. M. *J. Chem. Phys.* **1995**, *102*, 7035.
(61) *CRC Handbook of Chemistry and Physics*, 63rd ed.; Weast, R. C. Ed.; CRC Press: Boca Raton, 1982.
(62) Bhaduri, S.; Johnson, B. F. G.; Pickard, A.; Raithby, P. R.; Sheldrick, G. M.; Zuccaro, C. I. *J. Chem. Soc., Chem. Commun.* **1977**, 354.
(63) $[Cu(H_2O)_x]^{n+}$ and $[Cu(H_2O)_xNO]^{n+}$ geometries, which are the reference structures used for calculating the binding energies of the first and second NO, respectively, were obtained from ref 36 and reoptimized using the new set of criteria. The former complexes were constrained to C_{2v} symmetry ($x = 1,2$) or C_{4v} symmetry ($x = 4$), and the latter to C_s symmetry,[38] so that the NO ligands were free to bend in all cases (including $[Cu(H_2O)_xNO]^{2+}$ complexes, unlike in ref 36, where Cu−N−O was constrained to be linear); for this reason the binding energies of the first NO to $[Cu(H_2O)_x]^{2+}$ in Table 3 are slightly different from the corresponding values in ref 36.
(64) Enemark, J. H.; Feltham, R. D. *Coord. Chem. Rev.* **1974**, *13*, 339.
(65) Richter-Addo, G. B.; Legzdins, P. *Metal Nitrosyls*; Oxford University Press: Oxford, 1992.
(66) Water, J. M.; Whittle, K. R. *J. Chem. Soc., Chem. Commun.* **1971**, 518.
(67) Pierpont, C. G.; Van Derveer, D. G.; Durland, W.; Eisenberg, R. *J. Am. Chem. Soc.* **1970**, *92*, 4760.
(68) Eisenberg, R.; Mayer, C. A. *Acc. Chem. Res.* **1975**, *8*, 26.
(69) Greenwood, N. N.; Earnshaw, A. *Chemistry of the Elements*; Pergamon Press: New York, 1984.
(70) Partington, J. R.; Shah, C. C. *J. Chem. Soc.* **1931**, 2071.
(71) Oza, T. M.; Oza, V. T. *J. Chem. Soc.* **1953**, 909.
(72) Bhaduri, S.; Johnson, B. F. G.; Savory, C. J.; Segal, J. A.; Walter, R. H. *J. Chem. Soc., Chem. Commun.* **1974**, 809.
(73) Muccigrosso, D. A.; Mares, F.; Diamond, S. E.; Solar, J. P. *Inorg. Chem.* **1983**, *22*, 960.
(74) Kaneko, K.; Kobayashi, A.; Matsumoto, A.; Hotta, Y.; Suzuki, T.; Ozeki, S. *Chem. Phys. Lett.* **1989**, *163*, 61.
(75) Johnson, B. G.; Gill, P. M. W.; Pople, J. A. *J. Chem. Phys.* **1993**, *98*, 5612.
(76) Pearson, R. G. *Symmetry Rules for Chemical Reactions: Orbital Topology and Elementary Processes*; Wiley: New York, 1976.
(77) Cotton, F. A. *Chemical Applications of Group Theory*; 2nd ed.; Wiley-Interscience, New York, 1971; pp 178−193.
(78) Woodward, R. B.; Hoffmann, R. *Angew. Chem., Int. Ed. Engl.* **1969**, *8*, 781.
(79) That it is a quadruply excited state can be seen by rearranging the electrons in the left (and middle) of Figure 7 (thereby creating an excited state), so that levels of the same symmetry remain occupied on going to the right.
(80) Kersting, M.; Hoffmann, R. *Inorg. Chem.* **1990**, *29*, 279.
(81) Casewit, C. J.; Rappé, A. K. *J. Catal.* **1984**, *89*, 250.
(82) Schneider, W. F.; Hass, K. C.; Ramprasad, R.; Adams, J. B. *J. Phys. Chem. B* **1997**, *101*, 4353.